Int. J. Heat Mass Transfer. Vol. 36, No. 5, pp. 1295–1301, 1993
Printed in Great Britain

0017-9310/93 $6.00+0.00

Transient conjugated heat transfer in channel flows with convection from the ambient

WEI-MON YAN

Department of Mechanical Engineering, Fua-Han Institute of Technology, Shih Ting, Taipei, Taiwan 22305, R.O.C.

(*Received* 21 *February* 1992 *and in final form* 18 *June* 1992)

Abstract—This study presents a numerical solution of the transient conjugated heat transfer in a channel flow with convection from the ambient. The solution takes wall conduction and heat capacity effects into consideration. The effects of wall-to-fluid conductivity ratio K, the dimensionless wall thickness β, the wall-to-fluid thermal diffusivity ratio A and the outside Nusselt number Nu_0 on the interfacial heat flux, interfacial and bulk temperatures are discussed in detail. Results show that wall effect plays a significant role in the transient conjugated heat transfer problem. Particularly, the wall-to-fluid thermal diffusivity ratio A has a decisive effect with regard to the speed of propagation of thermal energy from the wall–fluid interface to the outer surface of the channel. In addition, the time required for heat transfer to reach the steady state condition is longer for systems with larger K and β or smaller A and Nu_0.

INTRODUCTION

CONSIDERABLE interest in unsteady characteristics of heat transfer equipment has been stimulated by the needs of modern technology, especially in relation to use of automatic control devices for accurate regulation of fluid systems involving heat exchange devices. In power plates the thermal transients resulting from unsteadiness in the thermal behavior can significantly affect their control systems. These transients may be accidental as in the case of power surge and pump failure, or they may be purposely introduced as in the case of a change in operating level occurring between different steady-state levels. In many events the control system associated with an apparatus must be planned with a knowledge of the effect of the thermal characteristics of its various components on the overall performance. Since heat transfer exchange equipment commonly consists of an assemblage of pipe or channel elements, one approach to study heat exchange dynamics is to investigate the unsteady behavior of a typical element, namely, a single passage and its boundary walls.

Most heat transfer problems involve an interaction of conduction in a solid wall and convection in an adjacent fluid. The spatial and temporal variations of the thermal conditions along the fluid–wall interface are then not known *a priori*, but what is known is a thermal boundary condition at some other surface of the solid wall. For such cases, it is necessary to solve the energy equations for the fluid and the solid wall under the conditions of continuity in the temperature and heat flux along the fluid–wall interface at every instant of time. Commonly, problems of this kind are referred to as the conjugated heat transfer problems.

Steady conjugated heat transfer in channel flow has been investigated by several investigators in the past two decades. For the case of a thermally inactive wall and a low Peclet number flow, the effect of axial conduction in the fluid was examined by a number of investigators, and the relevant literature has been brought together in Chapter 5 of ref. [1]. Wall conduction effects have been studied in refs. [2–4] for flows where there is no axial conduction in the fluid. The effects of the simultaneous axial conduction in the fluid and the wall were examined by Faghri and Sparrow [5], Wijeysundera [6] and Guedes *et al.* [7].

The simplest approach to the unsteady convection heat transfer in a channel is under the assumption of an extremely thin wall, i.e. effects of thermal capacity and resistance of solid wall can be neglected. The studies of the problem just mentioned were addressed in refs. [8–13]. The results of such investigations are only good for heat transfer in flows bounded by extremely thin walls. In practical situations the channel wall is normally finite in thickness, and thereby the thermal resistance associated with the conduction heat transfer in solid wall and the process of thermal energy storing in the wall during the transient state must be included in the analysis.

The influences of heat capacity of a duct wall on transient forced convection heat transfer in channel flows have been examined by Sucec [14–16], Cotta *et al.* [17], Li and Kakac [18] and Travelho and Santos [19]. These contributions showed that it is of great importance. Nevertheless, wall conduction still remained untreated. The latter effects were investigated by Lin and Kuo [20], Olek *et al.* [21] and Lee and Yan [22]. In these studies, the thermal condition of a step change in heat flux or wall temperature along the outer surface of a pipe wall is assumed.

The lack of information on unsteady conjugated

NOMENCLATURE

A	wall-to-fluid thermal diffusivity ratio, α_w/α_f
a	coefficient of finite difference form
b	half channel width [m]
c_{pf}	specific heat of fluid [kJ kg^{-1} K^{-1}]
c_{pw}	specific heat of solid wall [kJ kg^{-1} K^{-1}]
K	wall-to-fluid conductivity ratio, k_w/k_f
h_o	convective heat transfer coefficient outside wall [W m^{-2} K^{-1}]
i, j, k	indices in the axial direction, transverse direction and time step, respectively
k_f	thermal conductivity of fluid [W m^{-1} K^{-1}]
k_w	thermal conductivity of wall [W m^{-1} K^{-1}]
L	dimensionless cooling length, l/b
l	cooling length [m]
Nu_o	outside Nusselt number, $h_o \cdot b/k_f$
Pe	Peclet number, $4bu_e/\alpha_f$
Q_{wi}	dimensionless interfacial heat flux
T_e	inlet or initial temperature [K]
T_f	fluid temperature [K]
T_o	ambient temperature [K]
T_w	wall temperature [K]
t	time [s]
u_e	inlet fluid axial velocity [m s^{-1}]
u_{max}	axial centerline velocity
X	dimensionless axial coordinates, x/b
x	axial coordinate [m]
Y	dimensionless transverse coordinate, y/b
y	transverse coordinate [m].

Greek symbols

α_f	thermal diffusivity of fluid [m^2 s^{-1}]
α_w	thermal diffusivity of wall [m^2 s^{-1}]
β	dimensionless wall thickness, δ/b
δ	wall thickness [m]
θ_f	dimensionless fluid temperature, $(T_f-T_o)/(T_e-T_o)$
θ_b	dimensionless bulk temperature
θ_w	dimensionless wall temperature, $(T_w-T_o)/(T_e-T_o)$
θ_{wi}	dimensionless interfacial fluid–wall temperature
ρ_f	fluid density [kg m^{-3}]
ρ_w	wall density [kg m^{-3}]
τ	dimensionless time, $t/(b^2/\alpha_f)$.

Subscripts

b	bulk quantity
e	initial value at the entrance of the channel
f	fluid
w	wall
wi	fluid–wall interface.

heat transfer in channel flow motivates the present work. In this study, a numerical study is performed to investigate the effects of wall heat capacity and wall conduction on the transient heat transfer in a channel experiencing a sudden change in ambient temperature. The reason for considering a unit step change in ambient temperature instead of a unit step change in wall temperature or wall flux is a more practical situation and the solution is expected to be the same as that for wall temperature change while $Nu_o \to \infty$, and that for wall heat flux change while $Nu_o \to 0$ [6, 7, 16].

ANALYSIS

Consideration is given to an infinitely long channel ($-\infty < x < \infty$), with half channel width b and wall thickness δ. A schematic diagram of the present problem is depicted in Fig. 1. The fluid entering the channel has a uniform velocity u_e and temperature T_e in the far upstream end of the channel ($x \to -\infty$). The fluid, wall and ambient are considered to be initially isothermal with the entering fluid temperature identified as T_e. The channel is directly exposed to the ambient with an external heat transfer coefficient h_o over a finite length ($0 \leqslant x \leqslant l$) and is externally insulated both upstream ($-\infty < x < 0$) and downstream ($l < x < \infty$) of the channel. At time $t = 0$, the ambient temperature is suddenly changed to a new level T_o. Heat is transferred in the channel wall both upstream and downstream of the cooling section by axial conduction. Heat is transported to the solid wall by convection heat transfer at the solid–fluid interface. In the fluid domain, the heat is transferred in the direction of the flow by advection and conduction.

(A) *Governing equations*

Since the fluid is assumed to enter the channel in the far upstream region, the flow can be regarded as hydrodynamically fully developed in the region where

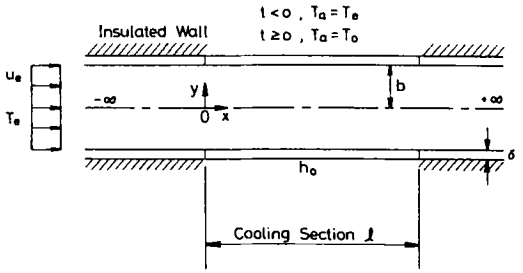

FIG. 1. Schematic model of parallel plate channel flow.

heat transfer is significantly present. By considering the thermophysical properties of the fluid and wall to be temperature independent, the energy transport processes in the problem treated can be formulated by the following non-dimensional equations:

Energy equation for the fluid

$$\frac{\partial\theta_f}{\partial\tau}+\tfrac{3}{8}Pe(1-Y^2)\cdot\frac{\partial\theta_f}{\partial X}=\frac{\partial^2\theta_f}{\partial X^2}+\frac{\partial^2\theta_f}{\partial Y^2}. \quad (1)$$

Energy equation for the wall

$$\frac{\partial\theta_w}{\partial\tau}=A\left[\frac{\partial^2\theta_w}{\partial X^2}+\frac{\partial^2\theta_w}{\partial Y^2}\right]. \quad (2)$$

(B) *Initial and boundary conditions*

The initial conditions are

$$\tau=0,\quad \theta_f=\theta_w=1,\quad -\infty<X<\infty. \quad (3)$$

The governing equations are subjected to the following boundary conditions:

$$Y=0,\quad \partial\theta_f/\partial Y=0,\quad -\infty<X<\infty \quad (4)$$

$$Y=1+\beta,\quad \partial\theta_w/\partial Y=\begin{cases}-Nu_o\cdot\theta_w/K, & 0<X<\infty\\ 0, & \text{otherwise}\end{cases} \quad (5)$$

$$X\to-\infty,\quad \theta_f=\theta_w=1 \quad (6)$$

$$X\to\infty,\quad \partial\theta_f/\partial Y=\partial\theta_w/\partial Y=0 \quad (7)$$

where the outside Nusselt number Nu_o in equation (5) is defined as [6, 7, 16]:

$$Nu_o=h_o\cdot b/k_f. \quad (8)$$

The conditions of the continuities in temperature and heat flux along the fluid–wall interface are

$$Y=1,\quad \theta_f=\theta_w \quad (9a)$$

$$\partial\theta_f/\partial Y=K\cdot\partial\theta_w/\partial Y \quad (9b)$$

where the dimensionless quantities are defined as

$$X=x/b,\qquad Y=y/b$$
$$\tau=t/(b^2/\alpha_f)\qquad L=l/b$$
$$K=k_w/k_f\qquad A=\alpha_w/\alpha_f$$
$$\beta=\delta/b,\qquad Pe=4u_eb/\alpha_f$$
$$\theta=(T-T_o)/(T_e-T_o). \quad (10)$$

The variables of engineering interest are the interfacial temperature, bulk fluid temperature and dimensionless interfacial heat flux. These variables are defined as follows:

$$\theta_{wi}=\theta_f(X,1)=\theta_w(X,1) \quad (11)$$

$$\theta_b=\int_0^1(1-Y^2)\theta_f\,dY\Big/\int_0^1(1-Y^2)\,dY \quad (12)$$

$$Q_{wi}=\partial\theta_f/\partial Y|_{Y=1}. \quad (13)$$

SOLUTION METHOD

Because of the complex interactions between the convection heat transfer in the flow and the conduction heat transfer in the channel wall across the fluid–wall interface, the solution of the problem defined by the foregoing equations can be better solved by the numerical finite-difference procedures. Since the governing equations, equations (1) and (2), are elliptic in space and parabolic in time, the solutions can be marched forward in time and swept in space from upstream to the downstream of the cooling region with iteration. For the purpose of numerical stability, a fully implicit formulation in time is adopted. The unsteady energy storage and advection terms are approximated by backward difference and upwind difference, respectively. The axial and transverse diffusion terms are approximated by the central difference. The matching condition imposed at the fluid–wall interface, equation (9b), so as to ensure the continuity of heat flux, was recast in backward difference for $\partial\theta_f/\partial Y$ and forward difference for $\partial\theta_w/\partial Y$. The solution to the energy equations both in the fluid and the channel wall can then be solved simultaneously by the line-by-line method [23]. Therefore, equations (1) and (2) can be written in the finite difference form:

$$a_{i2}\theta^m_{i,2}+a_{i3}\theta^m_{i,3}=a_{i4}+a_{i5}\theta^m_{i-1,1}+a_{i6}\theta^m_{i+1,1} \quad (14)$$

$$a_{j1}\theta^m_{i,j-1}+a_{j2}\theta^m_{i,j}+a_{j3}\theta^m_{i,j+1}=a_{j4}+a_{j5}\theta^m_{i-1,j}+a_{j6}\theta^m_{i+1,j} \quad (15)$$

$$a_{J1}\theta^m_{i,J-1}+a_{J2}\theta^m_{i,J}=a_{J4}+a_{J5}\theta^m_{i-1,J}+a_{J6}\theta^m_{i+1,J} \quad (16)$$

where $\theta^m_{i,j}$ is the dimensionless temperature difference at nodal point (i,j) at time m, and i, j and m are the indices in the axial direction, transverse direction and time, respectively. The a coefficients are omitted due to the space limit. Although the left-hand sides of the finite difference equations, equations (14)–(16), are written in tridiagonal form, in fact these finite difference equations are not tridiagonal as evident from the presence of the last terms on the right-hand sides. However, they can be solved by the Thomas algorithm [23], which is a very efficient numerical scheme for tridiagonal matrices, with iterations for each time step until a certain degree of convergence has been reached.

To obtain the desired accuracy, grids are non-uniformly spaced in the axial and transverse directions to account for the uneven variations of θ_f and θ_w. The grid point density is highest near the interface in the transverse direction, and concentration is highest in the neighborhood of $X=0$ and $X=L$ in the axial direction. In the transverse direction, the solid region $(1\leqslant Y\leqslant 1+\beta)$ was equally divided into 30 intervals, while in the fluid region $(0\leqslant Y\leqslant 1)$, 41 nodes were employed and successively enlarged by 5%. Axially, 151 nodal points are distributed in the domain of computation. The upstream, directly cooling, and downstream regions are, respectively, divided into 40, 40 and 70 intervals. The step size near the beginning

Table 1. Comparisons of local interfacial heat flux Q_{wi} for various grid arrangements for $K = 10$, $\beta = 0.2$, $A = 1$ and $Nu_o = 1$

$I \times J \times L$ / A	$301 \times 81 \times 61$		$151 \times 81 \times 61$		$151 \times 41 \times 31$		$76 \times 21 \times 16$	
τ	2.964	7.036	2.964	7.036	2.964	7.036	2.964	7.036
0.320	0.2217	0.2223	0.2212	0.2213	0.2210	0.2210	0.2257	0.2273
0.606	0.2506	0.2481	0.2502	0.2476	0.2502	0.2475	0.2512	0.2527
2.007	0.2530	0.1832	0.2529	0.1834	0.2528	0.1826	0.2508	0.1835
6.407	0.2576	0.1089	0.2557	0.1097	0.2548	0.1078	0.2480	0.1085
20.21	0.2516	0.1048	0.2504	0.1054	0.2488	0.1031	0.2404	0.1013
321.39	0.2478	0.1021	0.2456	0.1010	0.2458	0.1009	0.2387	0.0999

I = Number of grid points in the longitudinal direction.
J = Number of grid points in the transverse direction in the fluid side.
L = Number of grid points in the transverse direction in the wall side.

($X = 0$) and end ($X = L$) are smallest, and they are successively made larger by 5% in both positive and negative X directions. As far as the time step is concerned, the first time interval $\Delta\tau_1$ is taken to be 0.002 and every subsequent interval is enlarged by 10% over the previous one.

To validate the proposed numerical algorithm, the solution to the conjugated heat transfer in pipe flows subjected to a uniform heat flux was first obtained. The predicted interfacial heat flux is in excellent agreement with that of Lin and Kuo [20]. The result for a limiting case of steady-state conjugated heat transfer with convection from the ambient was also obtained. Good agreement with the results of Wijeysundera [6] and Guedes *et al.* [7] was found. Furthermore, to check the suitability of the finite-difference grid, the predicted interfacial heat flux Q_{wi} for a typical case from various grids at several time instants is compared in Table 1. It is clear in Table 1 that the differences in Q_{wi} for $301 \times 81 \times 61$ and $151 \times 41 \times 31$ grids are always less than 2%. Therefore the $151 \times 41 \times 31$ grid is considered to be suitable for the present study.

RESULTS AND DISCUSSION

Inspection of the preceding analysis reveals that the characteristics of transient conjugated heat transfer depend on six independent parameters, namely, the wall-to-fluid conductivity ratio K, the dimensionless wall thickness β, the wall-to-fluid thermal diffusivity A, the outside Nusselt number Nu_o, the Peclet number Pe, and the dimensionless cooling length L. While computations can be conducted for any combination of these parameters, the objective here is to present a simplification of the transient conjugated heat transfer which takes into account the heat capacity and wall conduction effects. In the following, both the cooling length L and Peclet number Pe are fixed to be 10.

Although the local Nusselt number is traditionally considered in the presentation of convective heat transfer results, the local Nusselt number is not a convenient design parameter in the study of conjugated heat transfer [16]. Instead, the interfacial heat flux distributions contain more meaningful information. The unsteady axial distributions of the interfacial heat flux Q_{wi} are shown in Fig. 2 for $K = 10$, $\beta = 0.2$, $A = 1$ and $Nu_o = 1$ at various instants of time. Inspection of Fig. 2 reveals that a substantial amount of heat flux occurs along the upstream of the cooling section. As expected, Q_{wi} curves drop off with increasing upstream distance. In the initial transient, only a small amount of energy is dissipated upstream. As time increases, the magnitude of heat flux becomes larger, and the thermal diffusion penetrates further upstream. In the directly cooling region ($0 \leqslant X \leqslant L$), Q_{wi} is small but rather uniform in the X direction during the early transient ($\tau \leqslant 0.320$). The small Q_{wi} is apparently due to the thermal lag of the system. The uniformity of Q_{wi} indicates that heat transfer in the flow is conduction-dominant at small τ. In fact, the time at which the heat transfer process at any position x is influenced by the convection of the fluid from the channel entrance is about x/u_{max}. In dimensionless variables, $t = x/u_{max}$, becomes $\tau = 8X/(3Pe)$. Hence, for $\tau = 0.32$, the conduction-dominated portion is limited to $X \geqslant 1.2$. Later ($\tau \geqslant 1.111$), convection in the flow becomes important and Q_{wi} is non-uniform in the X direction. Except in the region near the exit end of the cooling section ($X = L$), Q_{wi} in the cooling section gradually rises from zero to a maximum value with time. After reaching the maximum, Q_{wi} decreases until it reaches the steady-state value. In the neighborhood of the exit end of the cooling section, Q_{wi} shows a drastic change in the flow direction at different moments of time. Q_{wi} is positive when $\tau \leqslant 0.320$, but

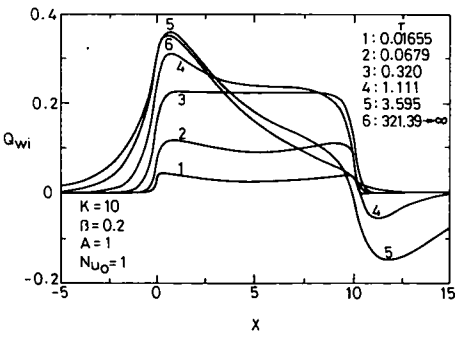

FIG. 2. Transient axial distributions of interfacial heat flux.

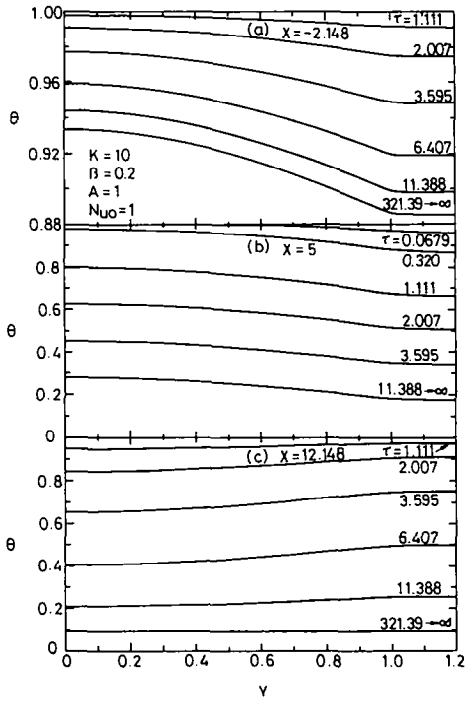

FIG. 3. Transient temperature profiles for various axial locations.

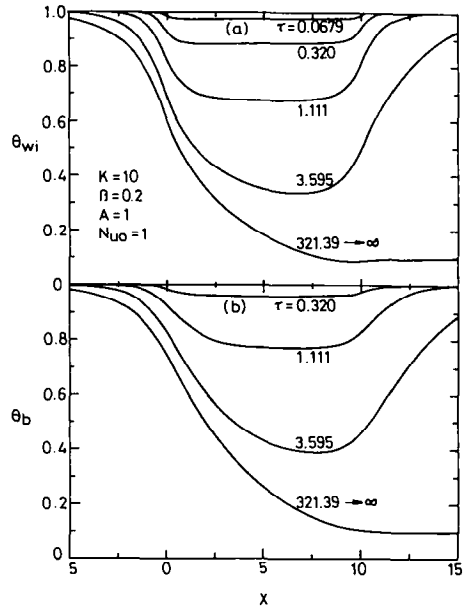

FIG. 4. Unsteady axial variations of interfacial and bulk temperatures.

becomes negative for $\tau \geqslant 1.111$, that is, heat transfer is now from the wall to the fluid. This reversal in heat transfer direction is caused by the conjugated nature of the wall conduction and flow convection processes. As τ is small, heat transfer is mainly confined in the wall region by conduction for $X \geqslant 3\tau \cdot Pe/8$. Hence the wall temperature is below the fluid temperature and heat transfer is from the fluid to the wall. At a later instant, convection in the flow becomes substantial and the fluid temperature is lower than the wall temperature resulting heat transfer from the wall to the fluid, as is evident in Fig. 3(c). For a large τ approaching the steady-state ($\tau \geqslant 321.39$), the wall temperature again is below the fluid temperature and heat transfer direction is then normal from the fluid to the wall. This complicated change in the wall and the fluid temperature with time in the downstream can be more clearly illustrated by the variations of temperature profiles given in Fig. 3(c). It is noteworthy in Fig. 3 that in the cooling section the temperature gets to the steady-state value quickly, relative to the upstream and downstream regions of the cooling section.

Aside from the interfacial heat flux which is an important aspect of thermal interactions between the fluid and the wall, the results for axial distributions of interfacial and bulk temperatures are more descriptive from the viewpoint of understanding the energy transport processes in the system. Hence, to improve our understanding, Fig. 4 gives the results for θ_{wi} and θ_b. As mentioned above, in the early transient period, the heat transfer mode is predominated by heat conduction. This causes flat curves of θ_{wi} and θ_b in the region of direct cooling. But the quantity of heat transported by axial conduction from the insulated section is very small so that the values of θ_{wi} and θ_b are small in the insulated portion near the entering end of the cooling section. With time elapsing, the effects of both the convection in the flow and the conduction in the wall increase, resulting in significant increases in θ_{wi} and θ_b at the initial portion of the region ($X \leqslant 0$). This portion gets larger with time.

To examine the influences of the wall-to-fluid conductivity ratio K, the axial distributions of Q_{wi}, θ_{wi} and θ_b are shown in Figs. 5 and 6 at various instants of time for $K = 1$. Particularly noticeable differences between Figs. 2 and 5 or Figs. 4 and 6 are that the heat penetration by the axial conduction in the channel wall becomes much smaller for $K = 1$ and the time period to get steady-state is much shorter for $K = 1$. This can be readily understood by recognizing that for a smaller K ($= A\rho_w c_{pw}/\rho_f c_{pf}$) with A fixed,

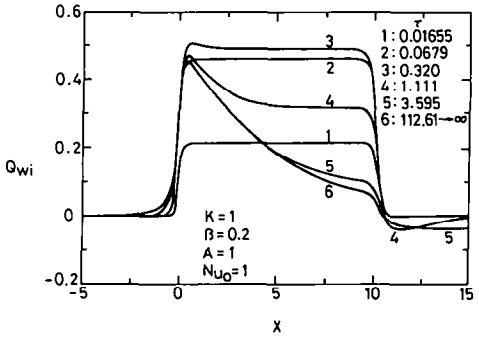

FIG. 5. Effects of the wall-to-fluid conductivity ratio K on the unsteady axial distributions of interfacial heat flux.

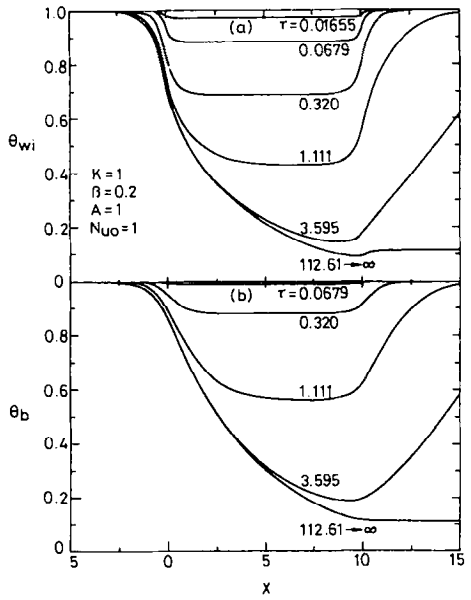

FIG. 6. Effects of the wall-to-fluid conductivity ratio K on the unsteady axial variations of interfacial and bulk temperatures.

the heat capacity for the wall $\rho_w c_{pw}$ is smaller by comparison with that for the fluid. Therefore a reduction in K results in less energy storage capacity of the solid wall and thus shortens the thermal lag in the system.

Next, the effects on the wall thickness β on the conjugated heat transfer are now examined. Figure 7 presents the predicted Q_{wi} with a thicker wall, $\beta = 0.5$. Comparison of Figs. 2 and 7 shows that when the wall becomes thicker, the heat penetration along the upstream end of the cooling section gets more significant because in this case larger cross-sectional area is provided for axial wall conduction. The energy storage capacity of the wall is larger for a larger β, causing the system to reach the steady state in a longer time period. In addition, it is found that the value of Q_{wi} at $\tau = 0.32$, when the heat conduction is still dominant, is larger for the case with a thinner wall ($\beta = 0.2$). The above outcomes are clearly due to the fact that the total thermal resistance and heat capacity of the wall

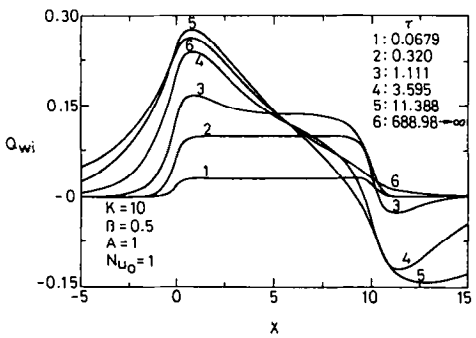

FIG. 7. Effects of the dimensionless wall thickness β on the unsteady axial distributions of interfacial heat flux.

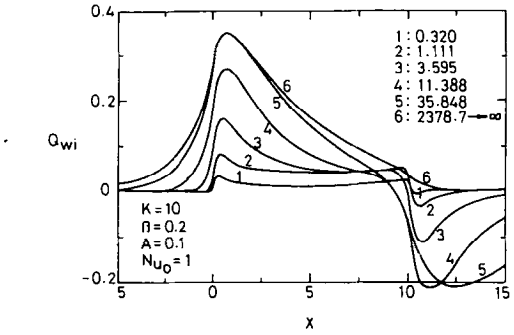

FIG. 8. Effects of the wall-to-fluid thermal diffusivity ratio A on the unsteady axial distributions of interfacial heat flux.

are smaller for a thinner wall so that the heat supplied from the wall–fluid interface is easily transported to the outer surface of the channel. Consequently, the presence of the channel wall has a prominent influence on the characteristics of unsteady heat transfer, and thus the wall effects cannot be neglected for transient heat transfer problems.

In Fig. 8, the effects of the wall-to-fluid thermal diffusivity ratio A on the distributions of Q_{wi} are given for $A = 0.1$ at various instants of time. These curves are very different from those in Fig. 2. Comparing the results in Figs. 2 and 8 indicates that a reduction in A from 1 to 0.1 results in a much larger thermal lag. This is due to the fact that for a smaller A ($=\alpha_w/\alpha_f$) heat diffusion in the wall is at a slower pace. Moreover, there is a significant difference between the results for Q_{wi} in Figs. 2 and 8—the magnitude of the negative Q_{wi} in the insulated portion near the exit end of the cooling section for the case with $A = 0.1$ is greater than that for the case with $A = 1$. The larger heat transfer reversal is due to the fact that for a smaller A the heat capacity of the wall is relatively larger, and thus the temperature penetration by axial conduction in the insulated solid wall to the adjacent cooling section is much slower than the energy transport by the forced convection from the flowing fluid in the cooling section. Note from these two figures that no matter what A is, the steady-state distributions of the interfacial heat flux are all the same.

The last parameter to be discussed is the outside Nusselt number Nu_o. Plotted in Fig. 9 are the dis-

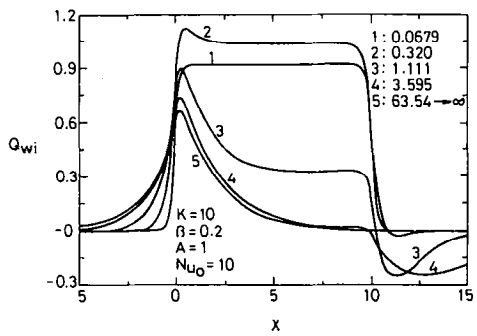

FIG. 9. Effects of the outside Nusselt number Nu_o on the unsteady axial distributions of interfacial heat flux.

tributions of Q_{wi} at various instants of time for $Nu_o = 10$. The curves are similar to those for $Nu_o = 1$ (Fig. 2). But there are noticeable differences between them. The time variations of Q_{wi} are more drastic for $Nu_o = 10$ at a given axial location. In addition, the flow reaches steady-state faster for $Nu_o = 10$. This is solely attributed to the increase in Nu_o which can enhance the transverse diffusion process.

Note that a quantitative criterion which indicates when one can safely neglect axial conduction within the wall and the fluid can be obtained from the results of the steady-state conjugated heat transfer. In ref. [1], it is pointed out that the axial conduction in the fluid can be ignored as the Peclet number Pe is greater than 100. Moreover, the results of Faghri and Sparrow [5] show that as $Pe \geqslant 50$, the effect of axial wall conduction on the interfacial heat transfer is negligible for $K \cdot \beta \leqslant 0.25$ under the thermal boundary condition of uniform wall heat flux.

CONCLUSIONS

Transient conjugated heat transfer in a channel with convection from the ambient has been numerically studied. The influences of the governing parameters, i.e. the wall-to-fluid conductivity ratio K, the dimensionless wall thickness β, the wall-to-fluid thermal diffusivity ratio A and the outside Nusselt number Nu_o, have been investigated in great detail. The major results can be briefly summarized as follows:

1. In the cooling section, the interfacial heat flux Q_{wi} rises from zero to a maximum value with an increase in time. After reaching the maximum, Q_{wi} decreases until it reaches the steady-state value. The unsteady variations of Q_{wi} considerably deviate from the corresponding steady-state values, especially in the initial transients.

2. The wall conduction plays a significant role in a transient conjugated heat transfer problem.

3. The time required for the heat transfer to reach the steady state condition is longer for the system with larger β and K or with smaller A and Nu_o.

4. The extent of the heat penetration in the upstream region of the cooling section increases with K and β.

5. In the design of heat exchangers operating at high pressures where channel walls need to be thick, one must account for the conjugated heat transfer phenomenon as well as the associated transients during startup or shutdown, or during a change in the operating conditions.

Acknowledgement—The financial support of this research by the Engineering Division of National Science Council, R.O.C., through the contract NSC81-0401-E211-502 is greatly appreciated.

REFERENCES

1. R. K. Shah and A. L. London, *Laminar Flow Forced Convection in Ducts*. Academic Press, New York (1978).
2. S. Mori, M. Sakakibara and A. Tamimoto, Steady heat transfer to laminar flow in a circular tube with conduction in the tube wall, *Heat Transfer—Jap. Res.* **3**, 37–46 (1974).
3. S. Mori, T. Shinke, M. Sakakibara and A. Tanimoto, Steady heat transfer to laminar flow between parallel plates with conduction in wall, *Heat Transfer—Jap. Res.* **5**, 17–25 (1976).
4. G. S. Barozzi and G. Pagliarini, A method to solve conjugate heat transfer problems: the case of fully developed laminar flow in a pipe, *J. Heat Transfer* **107**, 77–83 (1985).
5. M. Faghri and E. M. Sparrow, Simultaneous wall and fluid axial conduction in laminar pipe-flow heat transfer, *J. Heat Transfer* **102**, 58–63 (1980).
6. N. E. Wijeysundera, Laminar forced convection in circular and flat ducts with wall axial conduction and external convection, *Int. J. Heat Mass Transfer* **29**, 797–807 (1986).
7. R. O. C. Guedes, R. M. Cotta and N. C. L. Brum, Heat transfer in laminar flow with wall axial conduction and external convection, *J. Thermophys. Heat Transfer* **5**, 508–513 (1991).
8. R. Siegel, Transient heat transfer for laminar slug flow in ducts, *J. Appl. Mech.* **81**, 140–144 (1959).
9. M. Perlmutter and R. Siegel, Two-dimensional unsteady incompressible laminar duct flow with a step change in wall temperature, *Int. J. Heat Mass Transfer* **3**, 94–104 (1961).
10. H. T. Lin and Y. P. Shih, Unsteady thermal entrance heat transfer of power-law fluids in pipes and plate slits, *Int. J. Heat Mass Transfer* **24**, 1531–1539 (1981).
11. S. C. Chen, N. K. Anand and D. R. Tree, Analysis of transient convective heat transfer inside a circular duct, *J. Heat Transfer* **105**, 922–924 (1983).
12. T. F. Lin, K. H. Hawks and W. Leidenfrost, Unsteady thermal entrance heat transfer in laminar pipe flows with step change in ambient temperature, *Wärme- und Stoffübertragung* **17**, 125–132 (1983).
13. R. M. Cotta, M. N. Ozisik and D. S. McRae, Transient heat transfer in channel flow with step change in inlet temperature, *Numer. Heat Transfer* **9**, 619–630 (1986).
14. J. Sucec, Transient heat transfer in laminar thermal entrance region of a pipe: an analytic solution, *Appl. Sci. Res.* **43**, 115–125 (1986).
15. J. Susec, Exact solution for unsteady conjugated heat transfer in the thermal entrance region of a duct, *J. Heat Transfer* **109**, 295–299 (1987).
16. J. Susec, Unsteady conjugated forced convection heat transfer in a duct with convection from the ambient, *Int. J. Heat Mass Transfer* **30**, 1963–1970 (1987).
17. R. M. Cotta, M. D. Mikhailov and M. N. Ozisik, Transient conjugated forced convection in ducts with periodically varying inlet temperature, *Int. J. Heat Mass Transfer* **30**, 2073–2082 (1987).
18. W. Li and S. Kakac, Unsteady thermal entrance heat transfer in laminar flow with a periodic variation of inlet temperature, *Int. J. Heat Mass Transfer* **34**, 2581–2592 (1991).
19. J. S. Travelho and W. F. N. Santos, Solution for transient conjugated forced convection in the thermal entrance region of a duct with periodically varying inlet temperature, *J. Heat Transfer* **113**, 558–562 (1991).
20. T. F. Lin and J. C. Kuo, Transient conjugated heat transfer in fully developed laminar pipe flows, *Int. J. Heat Mass Transfer* **31**, 1093–1102 (1988).
21. S. Olek, E. Elias, E. Wacholder and S. Kaizerman, Unsteady conjugated heat transfer in laminar pipe flow, *Int. J. Heat Mass Transfer* **34**, 1443–1450 (1991).
22. K. T. Lee and W. M. Yan, Transient conjugated forced convection heat transfer with fully developed laminar flow in pipe, *Numer. Heat Transfer* (in press).
23. S. V. Patankar, *Numerical Heat Transfer and Fluid Flow*, Chapters 4 and 5. Hemisphere/McGraw-Hill, New York (1980).